Congenital bone marrow failure in DNA-PKcs mutant mice associated with deficiencies in DNA repair

Shichuan Zhang,[1] Hirohiko Yajima,[1] HoangDinh Huynh,[2] Junke Zheng,[2] Elsa Callen,[3] Hua-Tang Chen,[3] Nancy Wong,[3] Samuel Bunting,[3] Yu-Fen Lin,[1] Mengxia Li,[1] Kyung-Jone Lee,[1] Michael Story,[1] Eric Gapud,[4] Barry P. Sleckman,[4] André Nussenzweig,[3] Cheng Cheng Zhang,[2] David J. Chen,[1] and Benjamin P.C. Chen[1]

[1]Division of Molecular Radiation Biology, Department of Radiation Oncology, and [2]Department of Physiology, University of Texas Southwestern Medical Center, Dallas, TX 75390
[3]Experimental Immunology Branch, National Cancer Institute, National Institutes of Health, Bethesda, MD 20892
[4]Department of Pathology and Immunology, Washington University School of Medicine, St. Louis, MO 63110

The nonhomologous end-joining (NHEJ) pathway is essential for radioresistance and lymphocyte-specific V(D)J (variable [diversity] joining) recombination. Defects in NHEJ also impair hematopoietic stem cell (HSC) activity with age but do not affect the initial establishment of HSC reserves. In this paper, we report that, in contrast to deoxyribonucleic acid (DNA)–dependent protein kinase catalytic subunit (DNA-PKcs)–null mice, knockin mice with the DNA-PKcs$^{3A/3A}$ allele, which codes for three alanine substitutions at the mouse Thr2605 phosphorylation cluster, die prematurely because of congenital bone marrow failure. Impaired proliferation of DNA-PKcs$^{3A/3A}$ HSCs is caused by excessive DNA damage and p53-dependent apoptosis. In addition, increased apoptosis in the intestinal crypt and epidermal hyperpigmentation indicate the presence of elevated genotoxic stress and p53 activation. Analysis of embryonic fibroblasts further reveals that DNA-PKcs$^{3A/3A}$ cells are hypersensitive to DNA cross-linking agents and are defective in both homologous recombination and the Fanconi anemia DNA damage response pathways. We conclude that phosphorylation of DNA-PKcs is essential for the normal activation of multiple DNA repair pathways, which in turn is critical for the maintenance of diverse populations of tissue stem cells in mice.

Introduction

DNA double-stranded breaks (DSBs) are among the most dangerous forms of DNA damage. Unrepaired DSBs signal cells to die, whereas misprocessing of DSBs can lead to genomic instability and oncogenic transformation. DSBs are primarily repaired by the nonhomologous end-joining (NHEJ) and homologous recombination (HR) repair pathways. The NHEJ pathway joins the two ends of a DSB directly with little or no requirement for homology, whereas HR uses the intact identical copy of the broken chromosome as a template. Although both NHEJ and HR proteins are recruited to DSBs, pathway choice is regulated in part by the cell cycle phase, with HR being active in S/G2 and NHEJ contributing to DSB repair predominantly in G0/G1. For example, V(D)J (variable [diversity] joining) recombination-associated breaks are generated in G0/G1 and resolved by NHEJ proteins, whereas meiotic DSBs are processed by HR proteins. Nevertheless, a recent study indicates competition between HR and NHEJ for replication- and ionizing radiation (IR)–induced DSBs during the S and G2 phase of the cell cycle (Sonoda et al., 2006).

Correspondence to Benjamin P.C. Chen: benjamin.chen@utsouthwestern.edu

Abbreviations used in this paper: ATM, ataxia telangiectasia mutated; ATR, ATM and Rad3 related; BMT, bone marrow transplantation; DNA-PK, DNA-dependent protein kinase; DNA-PKcs, DNA-PK catalytic subunit; DR, direct repeat; DSB, double-stranded break; ES, embryonic stem; FA, Fanconi anemia; GR, glucocorticoid receptor; HR, homologous recombination; HSC, hematopoietic stem cell; IR, ionizing radiation; MEF, mouse embryonic fibroblast; MMC, mitomycin C; NHEJ, nonhomologous end joining; SCID, severe combined immunodeficiency; tACE, testes-specific angiotensin-converting enzyme.

The Rockefeller University Press $30.00
J. Cell Biol. Vol. 193 No. 2 295–305
www.jcb.org/cgi/doi/10.1083/jcb.201009074

The DNA-dependent protein kinase (DNA-PK) consists of the large catalytic subunit (DNA-PK catalytic subunit [DNA-PKcs]) and the DNA-binding Ku70/80 heterodimer. The DSB is initially recognized by DNA-PK. The ends are then synapsed and processed by other NHEJ proteins, including Artemis, XLF, and XRCC4, before they are ligated together by ligase IV (Weterings and Chen, 2008). DNA-PKcs belongs to a serine/threonine protein kinase family known as the phosphatidylinositol-3 kinase–like protein kinases. Family members include ataxia telangiectasia mutated (ATM) and ATM- and Rad3-related (ATR) kinases (Shiloh, 2003). DNA-PKcs, itself, is essential for NHEJ-mediated DSB repair, and loss of the DNA-PKcs protein leads to radiation hypersensitivity as well as severe combined immunodeficiency (SCID) caused by a block in V(D)J recombination. In addition, DNA-PKcs deficiency results in a defect in immunoglobulin class switch recombination (Manis et al., 2002; Cook et al., 2003; Callén et al., 2009). DNA-PKcs is phosphorylated in several regions in vitro upon activation and in vivo upon treatment with IR (Chan et al., 2002; Douglas et al., 2002; Chen et al., 2005; Ma et al., 2005; Meek et al., 2007). IR-induced Ser2056 phosphorylation is mediated by DNA-PKcs autophosphorylation, as it is significantly reduced in a kinase-dead mutant DNA-PKcs and is inhibited by the DNA-PKcs kinase inhibitor (Chen et al., 2005). In contrast, DNA-PKcs phosphorylation at the Thr2609 cluster is dependent on ATM and ATR kinases in response to IR and UV radiation, respectively (Yajima et al., 2006; Chen et al., 2007). DNA-PKcs phosphorylation at either the Thr2609 cluster or at Ser2056 does not affect its kinase activity; nevertheless, abrogation of DNA-PKcs phosphorylation at either region attenuates DSB repair and leads to increased radiosensitivity (Chan et al., 2002; Ding et al., 2003; Chen et al., 2005, 2007).

To gain insight into the physiological significance of phosphorylation at this cluster, we have generated a 3A knockin mouse model, in which the three threonine residues are substituted with alanines. In this study, we report that DNA-PKcs$^{3A/3A}$ mice surprisingly develop congenital hematopoietic failure caused by rapid loss of hematopoietic stem cells (HSCs) in the developing fetal liver. This severe hematopoietic phenotype was attributed to a compound deficiency in DSB repair, including the HR and Fanconi anemia (FA) pathways. Because being defective in NHEJ alone does not block HSC expansion in the embryo, we conclude that the HR/FA pathways are essential for HSC development and that DNA-PKcs phosphorylation at the Thr2609 cluster is a prerequisite for the pathway switch favoring HR/FA.

Results

Generation of a DNA-PKcs^{3A} knockin mouse model

Our knockin mouse model of DNA-PKcs harbors three alanine substitutions at Thr2605, Thr2634, and Thr2643 (3A mutation, corresponding to human Thr2609, Thr2638, and Thr2647) of the endogenous mouse *DNA-PKcs* or *PRKDC* gene locus (Fig. 1 A). The design of the 3A knockin targeting vector was based on a previously described self-excision ACN (testes-specific angiotensin-converting enzyme [tACE]–Cre/neomycin [Neo]) cassette strategy (Bunting et al., 1999). The ACN cassette, including a testes-specific tACE promoter-driven Cre recombinase, a Neo-selectable marker, and two flanking loxP sites, was fused with two genomic fragments with the longer fragment carrying mutated exon 58 (covering the entire mouse Thr2605 cluster) in close proximity to the ACN cassette (Fig. 1 B). Upon successful gene targeting and subsequent germline transmission in chimeric mice, expression of Cre recombinase during spermatogenesis self-excises the ACN cassette. This process leaves behind one remaining loxP site and allows the expression of the 3A mutant DNA-PKcs from the targeted allele. Using this strategy, two knockin mouse lines were generated from two independently targeted embryonic stem (ES) cell clones. Analyses of mice and cultured cells yielded identical phenotypes from both lines.

Alanine substitutions at all three threonine sites (Thr2605, Thr2634, and Thr2643) of the targeted allele were confirmed by sequencing DNA isolated from tails of heterozygotic (DNA-PKcs$^{+/3A}$) carriers. The sequencing profile showed equal detection of A from the wild-type allele and G from the targeted allele at all three mutated positions (Fig. S1 A). The 3A substitution and

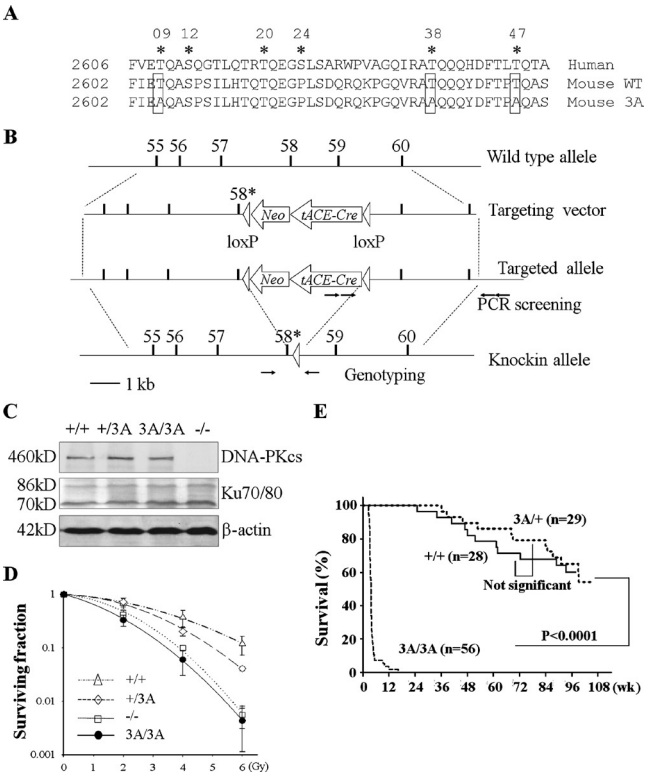

Figure 1. **Generation of a DNA-PKcs$^{3A/3A}$ knockin mouse model.** (A) The alignment of the human Thr2609 and the mouse Thr2605 phosphorylation cluster of DNA-PKcs. Six phosphorylation sites were identified in the human Thr2609 cluster (highlighted with asterisks), which are highly conserved in the mouse except for Ser2624. Boxes indicate the positions of knockin mutations or alanine substitutions. (B) Strategy to introduce knockin mutations into a mouse ES cell. 58*, exon 58 with T2605A, T2634A, and T2643A mutations; tACE-Cre, Cre recombinase driven by a tACE promoter. (C) 3A mutation does not alter the expression of DNA-PKcs. Whole-cell lysates from different MEFs were analyzed for the expression of DNA-PKcs, Ku70/80, and β-actin. (D) DNA-PKcs$^{3A/3A}$ MEFs are hypersensitive to radiation (representative of three independent assays). Error bars represent SD. (E) Survival curves generated by Kaplan–Meier analysis (curves were compared using log-rank test).

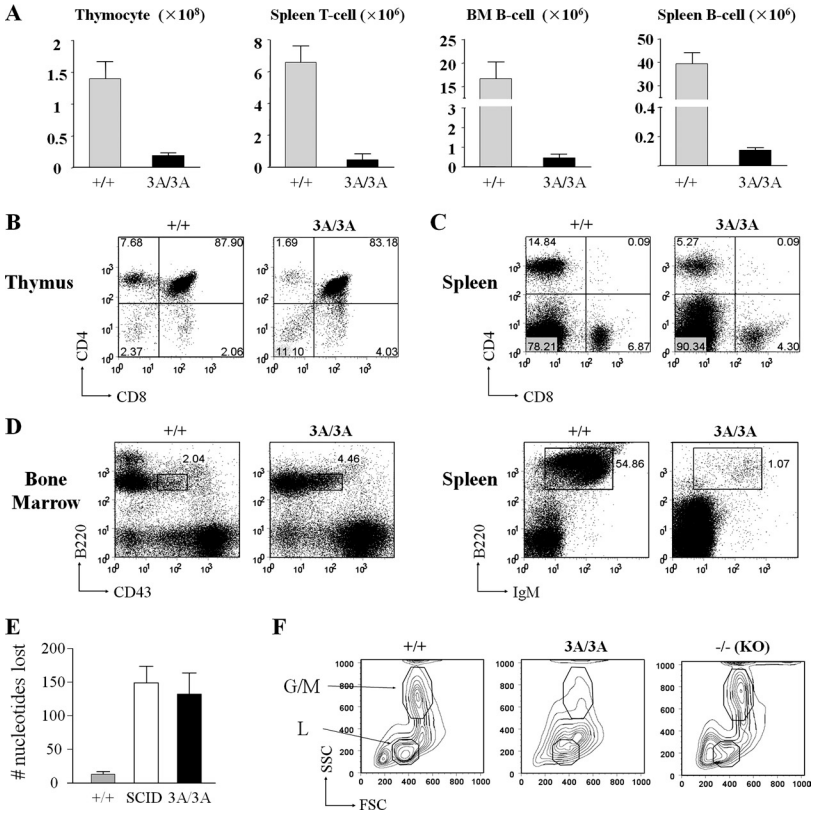

Figure 2. **Lymphocyte development in DNA-PKcs$^{3A/3A}$ mice.** (A) T and B cell numbers are drastically reduced in 2-wk-old DNA-PKcs$^{3A/3A}$ mice. $n = 4$. Error bars represent SD. (B) Flow cytometric analysis of thymocytes from 2-wk-old mice. Similar to wild-type cells, the majority of DNA-PKcs$^{3A/3A}$ thymocytes were double positive (CD4$^+$CD8$^+$). However, single-positive cell, particularly CD4$^+$CD8$^-$, thymocytes were reduced in DNA-PKcs$^{3A/3A}$ mice. (C) Flow cytometric analysis of splenocytes from 2-wk-old mice. Single-positive CD4$^+$CD8$^-$ and CD4$^-$CD8$^+$ T cells were present in the DNA-PKcs$^{3A/3A}$ spleen, but the numbers were also reduced. The numbers indicate the percentages of cell counts to total population in each quadrant. The lines separate the negative and the positive cell populations in each FACS analysis. (D) Flow cytometric analysis of B lymphocyte development. B cell development in DNA-PKcs$^{3A/3A}$ mice was arrested at the pro-B cell (B220^{low}CD43$^+$IgM$^-$) stage with very few mature B cells. Boxes indicate pro-B cell gate (B220^{low}CD43$^+$IgM$^-$); numbers indicate percentages of cells in the gate to total population. (E) Analysis of the mean number of junctional nucleotides lost in Dδ2:Jδ1 coding joints cloned and sequenced from wild-type, SCID, and DNA-PKcs$^{3A/3A}$ thymocytes. Means ± SEM are plotted for each genotype. Results from two mice were pooled for each genotype. Primary data are shown in Table S1, Table S2, and Table S3. (F) Side scatter (SSC) and forward scatter (FSC) signal of bone marrow (BM) cells in flow cytometric analysis. Data show that, in the DNA-PKcs$^{3A/3A}$ bone marrow, not only in the lymphoid (L) gate but also in the granulocyte and macrophage (G/M) gate, cell number dropped to a very low level compared with wild-type and knockout (KO) mice.

the one remaining loxP site between exon 58 and exon 59 did not affect the expression of the 3A mutant DNA-PKcs from the targeted allele, as similar levels of the DNA-PKcs protein were detected in mouse embryonic fibroblasts (MEFs) derived from all genotypes (Fig. 1 C). The 3A substitution also did not affect the kinase activity of DNA-PKcs (Fig. S1 D) as previously reported (Ding et al., 2003; Chen et al., 2007). Nonetheless, clonogenic survival analysis revealed that DNA-PKcs$^{3A/3A}$ MEFs were hypersensitive to IR to a similar degree as DNA-PKcs–null MEFs (Fig. 1 D).

Complete disruption of the mouse *DNA-PKcs* gene results in an SCID phenotype (Gao et al., 1998; Taccioli et al., 1998; Kurimasa et al., 1999), but in contrast to Ku-deficient mice, there is no apparent growth retardation, infertility, or life shortening in DNA-PKcs$^{-/-}$ mice (Nussenzweig et al., 1996; Gu et al., 1997; Ouyang et al., 1997). Homozygous DNA-PKcs$^{3A/3A}$ mice were born at the expected Mendelian frequency with similar body weight to littermates, but they became apparently smaller within 2–3 wk of age (Fig. S1 C). In striking contrast to the normal life span of control, heterozygous littermates, and DNA-PKcs$^{-/-}$ mice, the great majority of DNA-PKcs$^{3A/3A}$ mice died shortly after birth (Fig. 1 E). In a cohort of 56 DNA-PKcs$^{3A/3A}$ mice, 75% died within 4 wk of birth, and only one mouse survived >12 wk.

Lymphocyte hypoplasia and the V(D)J recombination defect in DNA-PKcs$^{3A/3A}$ mice

Lymphocyte development in DNA-PKcs–null mice is severely compromised because of a block in V(D)J recombination (Gao et al., 1998; Taccioli et al., 1998; Kurimasa et al., 1999). Like DNA-PKcs$^{-/-}$ mice, the number of lymphocytes and the size of lymphoid organs were drastically attenuated in 2-wk-old DNA-PKcs$^{3A/3A}$ mice (Fig. 2 A and Fig. S2 A). In contrast to the early T cell development block at the CD4$^-$CD8$^-$ double-negative stage in DNA-PKcs–null mice (Gao et al., 1998; Kurimasa et al., 1999), DNA-PKcs$^{3A/3A}$ mice have CD4$^+$CD8$^+$, CD4$^+$CD8$^-$, and CD4$^-$CD8$^+$ thymocytes, although at significantly reduced numbers (Fig. 2, A and B). Analyses of thymocyte subsets also reveal a severe reduction of DNA-PKcs$^{3A/3A}$ double-negative thymocytes at different developmental stages (Fig. S2 B). Moreover, there is a significant reduction in the numbers of T cells expressing TCR-γ/δ (Fig. S2 C) and TCR-β (Fig. S2 D), which is observed in mice with mutations that cause a subtotal block in V(D)J recombination (Difilippantonio et al., 2008). Nevertheless, single-positive splenic T cells accumulated in the DNA-PKcs$^{3A/3A}$ spleen (Fig. 2 C). B cell development in DNA-PKcs$^{3A/3A}$ mice was also dramatically affected, with an apparent arrest at the B220^{low}CD43$^+$IgM$^-$ (pro-B cell) stage in bone marrow and few mature B cells in the spleen (Fig. 2 D), which is similar to the defective B cell development in DNA-PKcs$^{-/-}$ mice (Gao et al., 1998; Taccioli et al., 1998; Kurimasa et al., 1999). Significant loss of nucleotides is a hallmark of coding joint formation in DNA-PKcs–deficient mice, and we find that the extent of nucleotide loss during coding joint formation in DNA-PKcs$^{3A/3A}$ thymocytes is similar to that observed in DNA-PKcs–deficient (SCID) thymocytes (Fig. 2 E, Fig. S2 E, Table S1, Table S2, and Table S3). Thus, phosphorylation of the Thr2605 cluster in DNA-PKcs is required for normal V(D)J recombination.

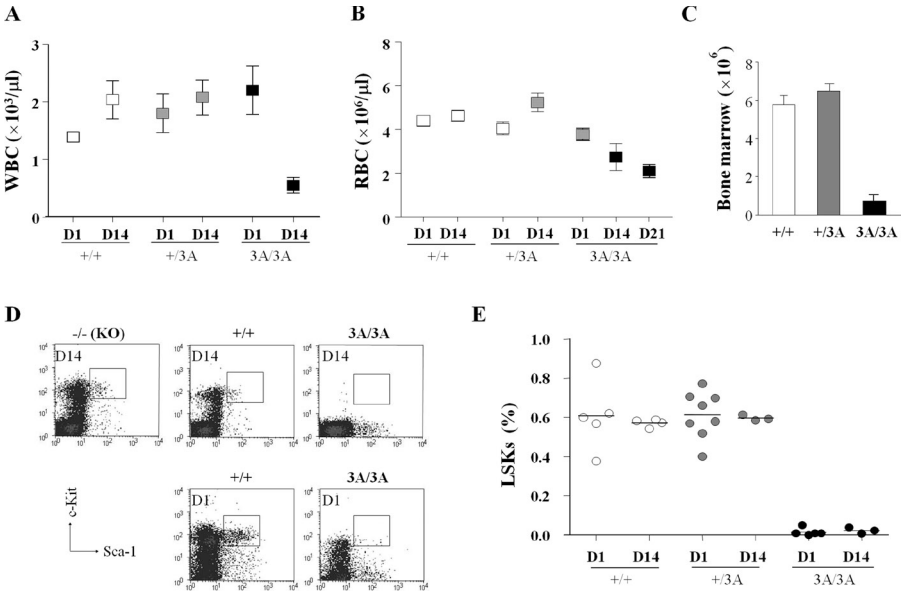

Figure 3. **Congenital bone marrow failure and HSC/progenitor cell depletion in DNA-PKcs$^{3A/3A}$ mice.** (A) The averages of peripheral blood WBC counts at day 1 (D1) and day 14 (D14) after birth (n = 4 for each group). (B) The averages of RBC counts reveal the development of anemia in DNA-PKcs$^{3A/3A}$ mice after birth (n = 4 for each group). (C) Bone marrow was depleted in DNA-PKcs$^{3A/3A}$ mice. Bone marrow was taken from one femur and one tibia of 2-wk-old mice (n = 3 for each group). Error bars represent SD. (D) Flow cytometric analysis of HSC-enriched LSK cells. Bone marrow cells were stained with a lineage marker cocktail, c-Kit, and Sca-1. LSK cells (Lin$^-$Sca-1$^+$c-Kit$^+$) and myeloid progenitor cells (Lin$^-$Sca-1$^-$c-Kit$^+$) were ablated in 2-wk-old (day 14) DNA-PKcs$^{3A/3A}$ mice. In newborn mice (day 1), myeloid progenitor cells were detected. Boxes indicate the LSK cell gate (Lin$^-$Sca-1$^+$c-Kit$^+$). (E) Quantification of flow cytometric analysis of HSCs ($n \geq 3$ for each group). Lines indicate the means for each group.

Congenital bone marrow failure and HSC loss in DNA-PKcs$^{3A/3A}$ mice

Although lymphocyte development is compromised in DNA-PKcs$^{3A/3A}$ mice, this would not be expected to cause early postnatal lethality in DNA-PKcs$^{3A/3A}$ mice, as SCID mice live a normal life span. Examination of forward angle versus side angle light scatter plots in bone marrow revealed not only a depletion of cells in the lymphocyte gate (as in SCID mice) but also a lack of cells in the granulocyte and macrophage gate in DNA-PKcs$^{3A/3A}$ bone marrow with a characteristically high level of side scatter, suggesting a more general loss of leukocytes (Fig. 2 F). During our investigation, we noticed that the ears, paws, and internal organs of DNA-PKcs$^{3A/3A}$ mice were pale, suggesting the development of anemia. A complete peripheral blood cell count in 2-wk-old mice revealed a significant reduction in the numbers of WBCs, RBCs, and platelets in DNA-PKcs$^{3A/3A}$ mice, suggesting the development of multilineage peripheral blood cytopenia (Table S4). Analysis of peripheral blood samples taken at different time points showed that pancytopenia in DNA-PKcs$^{3A/3A}$ mice began 2 wk after birth and worsened with age (Fig. 3, A and B). Consistent with the pancytopenia phenotype, the average number of bone marrow–nucleated cells in 2-wk-old DNA-PKcs$^{3A/3A}$ mice was significantly reduced (Fig. 3 C). These results suggest that depletion of bone marrow–nucleated cells in DNA-PKcs$^{3A/3A}$ mice leads to pancytopenia, which has not been observed in DNA-PKcs$^{-/-}$ or SCID mice.

Peripheral blood cells are continuously replenished from HSC pools in hematopoietic organs, particularly in postnatal bone marrow (Kondo et al., 2003). To examine whether a defect in HSC homeostasis was the cause of bone marrow depletion in DNA-PKcs$^{3A/3A}$ mice, a population of bone marrow HSCs (Lin$^-$Sca-1$^+$c-Kit$^+$, hereafter referred to as LSK cells) was evaluated by flow cytometric analysis (Morrison et al., 1995). The experiments revealed that bone marrow LSK cells and their derivative Lin$^-$Sca-1$^-$c-Kit$^+$ progenitor cells were almost ablated in 2-wk-old DNA-PKcs$^{3A/3A}$ mice and were 100 times less than wild type even at day 1 (Fig. 3, D and E), whereas no significant difference was found in wild type, DNA-PKcs$^{+/3A}$ mice (Fig. 3 E), or in DNA-PKcs$^{-/-}$ mice (Fig. 3 D). These results demonstrate that there is an impaired maintenance or self-renewal of bone marrow HSCs in DNA-PKcs$^{3A/3A}$ mice and that the initiation of HSC pathogenesis occurs during embryonic development. Importantly, this dramatic early HSC failure has not been observed in other NHEJ-deficient mouse strains, in which HSC reserves are generally preserved in young mice (Nijnik et al., 2007; Rossi et al., 2007).

Fetal liver HSC dysfunction and loss in DNA-PKcs$^{3A/3A}$ mice

The fetal liver is known to be the main source of hematopoiesis during embryonic development, as it provides supportive niches for HSC expansion and maturation (Mikkola and Orkin, 2006). To determine when HSC homeostasis dysfunction occurred in DNA-PKcs$^{3A/3A}$ embryos, fetal liver samples from different developmental stages were harvested and analyzed. Flow cytometric analysis revealed a decreased number of fetal liver LSK cells in DNA-PKcs$^{3A/3A}$ embryos at embryonic day (E) 14.5 (0.08 ± 0.04% vs. wild type 0.19 ± 0.06%) and E.16.5 (0.05 ± 0.02% vs. wild type 0.14 ± 0.02%; Fig. 4, A and B). At E12.5, the LSK cell population in DNA-PKcs$^{3A/3A}$ embryos was slightly reduced (0.23 ± 0.10%) but remained within the normal range of wild-type embryos (0.26 ± 0.11%; Fig. 4 B). Significantly, the depletion of HSC reserves in the DNA-PKcs$^{3A/3A}$ fetal liver occurs when HSCs are highly proliferative and undergo rapid expansion (Mikkola and Orkin, 2006). To examine whether the HSC loss in DNA-PKcs$^{3A/3A}$ mice was a result of defective cell proliferation, freshly isolated fetal liver LSK cells were cultured for ex vivo expansion. Wild-type and DNA-PKcs$^{+/3A}$ LSK cells proliferated exponentially and continuously during the course of ex vivo expansion, whereas DNA-PKcs$^{3A/3A}$ LSK cells proliferated normally only in the first 24 h (Fig. 4 C). The expansion of DNA-PKcs$^{3A/3A}$ LSK cells slowed down at 48 h and then collapsed at 72 h as a result of massive cell death (unpublished data).

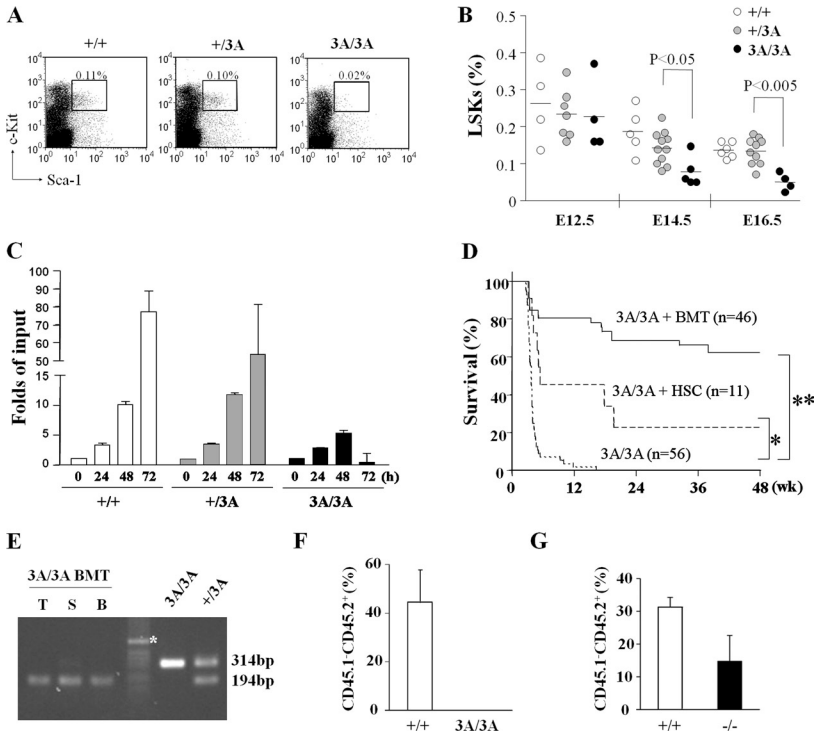

Figure 4. **Loss of fetal liver HSCs in DNA-PKcs$^{3A/3A}$ embryos.** (A) Flow cytometric analysis of HSC-enriched LSK cells in the E16.5 fetal liver. Percentages of LSKs are indicated. Boxes indicate the LSK cell gate (Lin$^-$Sca-1$^+$c-Kit$^+$). (B) Quantitative analysis of fetal liver LSKs. Data show progressive LSK loss in DNA-PKcs$^{3A/3A}$ embryos (one dot represents one sample; at least four samples from one time point were analyzed for each genotype). Lines indicate the means for each group. (C) Ex vivo expansion of E13.5 fetal liver LSK cells. DNA-PKcs$^{3A/3A}$ LSKs showed limited proliferation capacity compared with wild-type and DNA-PKcs$^{+/3A}$ LSKs. ($n = 3$ for each group). (D) Kaplan–Meier survival curves for untreated DNA-PKcs$^{3A/3A}$ mice, bone marrow–transplanted (BMT) DNA-PKcs$^{3A/3A}$ mice, and LSK cell–transplanted DNA-PKcs$^{3A/3A}$ mice (*, $P < 0.05$; **, $P < 0.001$; log-rank test). (E) Hematopoietic reconstitution in DNA-PKcs$^{3A/3A}$ BMT mice by donor cells. DNA samples from the thymus (T), spleen (S), and bone marrow (B) of DNA-PKcs$^{3A/3A}$ BMT mice were PCR genotyped. Wild-type PCR products were predominantly presented in all three tissues. The asterisk denotes a 517-bp band of the 1-kb DNA ladder (Invitrogen). (F) Competitive repopulation assay using E13.5 fetal liver cells. DNA-PKcs$^{3A/3A}$ HSCs (CD45.1$^-$CD45.2$^+$) failed to repopulate in lethally irradiated B6-LY5.2/Cr host mice (CD45.1$^+$CD45.2$^-$). $n = 4$. (G) Competitive repopulation was performed using bone marrow cells from 8-mo-old DNA-PKcs$^{-/-}$ and age-matched wild-type mice. DNA-PKcs$^{-/-}$ HSCs (CD45.1$^-$CD45.2$^+$) showed reduced repopulating potential. $n = 4$. Error bars represent SD.

Bone marrow transplantation rescues DNA-PKcs$^{3A/3A}$ mice

Defective HSC expansion in fetal liver and depletion of nucleated cells in postnatal bone marrow suggest that HSC failure might be the cause of early lethality in DNA-PKcs$^{3A/3A}$ mice. To test this hypothesis, bone marrow transplantation (BMT) was performed in 2-wk-old DNA-PKcs$^{3A/3A}$–recipient mice using wild-type littermates as donors. BMT was performed without preconditioning procedures because DNA-PKcs$^{3A/3A}$ mice are highly sensitive to radiation treatment (unpublished data) and are immunoincompetent. After transplantation with wild-type bone marrow cells, DNA-PKcs$^{3A/3A}$ recipients had an 80% survival rate at 2 mo and 60% at 1 yr (Fig. 4 D). BMT-rescued DNA-PKcs$^{3A/3A}$ mice gained weight normally compared with their heterozygotic littermates (Fig. S3 B). 8 wk after transplantation, peripheral blood cell counts in recipient mice showed a complete recovery from pancytopenia and the restoration of the bone marrow HSC pool (Fig. S3 A). Importantly, PCR genotyping revealed that hematopoietic organs in DNA-PKcs$^{3A/3A}$ recipients were reconstituted primarily by wild-type donor cells (Fig. 4 E), indicating a successful hematopoietic reconstitution. The rescue of DNA-PKcs$^{3A/3A}$ mice could also be achieved by transplantation with bone marrow LSK cells from wild-type littermates with a reduced efficiency (Fig. 4 D), as the LSK faction primarily contains the upstream HSCs. In contrast, bone marrow contains HSCs, progenitors, and partially differentiated progenitors for different hematopoietic lineages and is able to achieve a significant rescue within a shorter window of opportunity than LSKs.

The success of BMT rescue confirmed that HSC failure is the main cause of early lethality in DNA-PKcs$^{3A/3A}$ mice. To determine whether there is an intrinsic defect of DNA-PKcs$^{3A/3A}$ HSC proliferation in vivo, competitive repopulating assays were performed in irradiated CD45.1-recipient mice transplanted with fetal liver LSK cells from wild-type or DNA-PKcs$^{3A/3A}$ embryos (CD45.2 background) as well as the competing wild-type CD45.1 bone marrow cells. As shown in Fig. 4 F, DNA-PKcs$^{3A/3A}$ fetal liver LSKs were completely unable to repopulate in vivo, demonstrating the severity of hematopoietic impairment in DNA-PKcs$^{3A/3A}$ mice. In contrast, bone marrow cells from 8-mo-old DNA-PKcs$^{-/-}$ mice retained the reconstitution ability, though with a reduced potential compared with age-matched wild-type bone marrow cells (Fig. 4 G), suggesting a possible age-associated defect in hematopoiesis in DNA-PKcs$^{-/-}$ mice as also observed in other NHEJ-defective mice (Nijnik et al., 2007; Rossi et al., 2007).

Increase of spontaneous DNA lesions and apoptosis in DNA-PKcs$^{3A/3A}$ fetal liver HSCs

Based on our results, we hypothesized that the 3A mutant DNA-PKcs might interfere with endogenous DSB repair, resulting in an increase of spontaneous DNA lesions and cell death. To investigate this possibility, freshly isolated LSK cells from E12.5 fetal livers were stained for γ-H2AX nuclear foci, a commonly used surrogate marker of DSB formation. LSK cells isolated from wild-type and heterozygotic embryos rarely displayed γ-H2AX foci, and no more than five γ-H2AX foci were observed in individual wild-type cells, whereas the majority of DNA-PKcs$^{3A/3A}$ LSK cells were positively stained with γ-H2AX, and >30% contained more than five γ-H2AX foci (Fig. 5 A). In addition, a single-cell comet assay performed under alkaline conditions also revealed that a significant portion of DNA-PKcs$^{3A/3A}$ LSK cells contained the comet tail as compared with that of wild-type and heterozygotic LSK cells (Fig. S4 A). Consistent with the induction of spontaneous DNA lesions, an

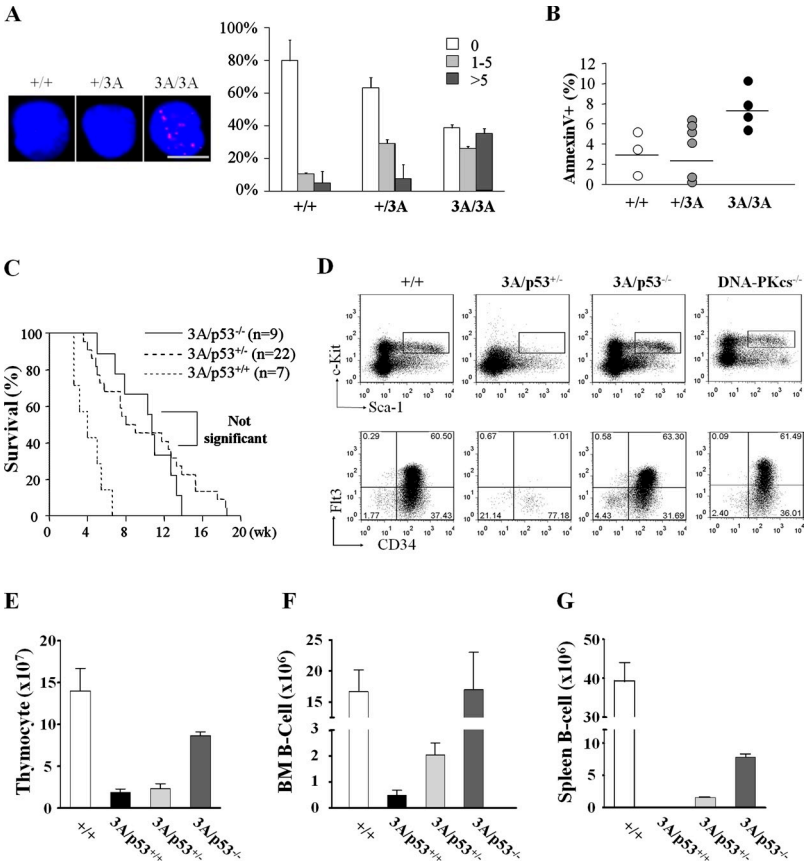

Figure 5. **Elevation of DNA damage and p53 signaling in DNA-PKcs$^{3A/3A}$ mice.** (A) γ-H2AX foci analysis with freshly isolated E12.5 fetal liver LSK cells. Cells were grouped into three categories based on the number of γ-H2AX foci: negative (zero foci/cell), positive (one to five foci/cell), and strong positive (more than five foci/cell). A total of 50 cells were randomly selected from each genotype for analysis. Data represent two independent assays. Bar, 10 µm. (B) Annexin V staining of freshly isolated LSKs from E13.5 fetal livers ($n \geq 3$ for each group). Lines indicate the means for each group. (C) Kaplan–Meier survival curves of DNA-PKcs$^{3A/3A}$ mice (abbreviated as 3A) in different p53 genotype backgrounds. (D) Flow cytometric analysis of bone marrow (BM) HSCs in 2-wk-old mice. HSC loss, particularly long-term HSC (Lin$^-$Sca-1$^+$c-Kit$^+$Flt3$^-$CD34$^-$) loss in DNA-PKcs$^{3A/3A}$ was completely rescued in the p53-null background. (top) Boxes indicate the LSK cell gate (Lin$^-$Sca-1$^+$c-Kit$^+$). (bottom) The numbers indicate the percentages of cell counts to total population in each quadrant. The lines separate the negative and the positive cell populations in each FACS analysis. (E–G) Null mutation of p53 rescues the numbers of T and B cells in DNA-PKcs$^{3A/3A}$ mice. The numbers of thymocytes (E), bone marrow B cells (F), and splenic B cells (G) were determined from 2-wk-old wild-type mice as well as in DNA-PKcs$^{3A/3A}$ mice with different p53 genotypes ($n \geq 3$ for each group). Error bars represent SD.

increase of Annexin V staining was also confirmed in freshly isolated fetal liver LSK cells from DNA-PKcs$^{3A/3A}$ embryos (Fig. 5 B), suggesting that HSC loss in DNA-PKcs$^{3A/3A}$ mice is likely caused by excessive apoptotic cell death.

Loss of p53 mitigates the stem cell failure and promotes survival in DNA-PKcs$^{3A/3A}$ mice

To examine whether HSC loss is caused by p53-mediated apoptotic response, DNA-PKcs^{3A} mice were crossed with p53-null mutant mice. Loss of both p53 alleles doubled the life span of homozygotic DNA-PKcs$^{3A/3A}$ mice (abbreviated as 3A; Fig. 5 C) and restored long-term HSCs (Lin$^-$Sca-1$^+$c-Kit$^+$Flt3$^-$CD34$^-$) in DNA-PKcs$^{3A/3A}$ mice (Fig. 5 D). Strikingly, loss of a single copy of p53 also prolonged the survival of 3A/p53$^{+/-}$ mice. In a cohort of 22 3A/p53$^{+/-}$ mice, 50% survived beyond 8 wk, which is significantly longer ($P < 0.001$) than the survival of 3A mice. Despite the enhanced survival, there was still a major depletion of bone marrow stem cells in 3A/p53$^{+/-}$ mice. We estimate from two femur bones that there are $\sim 4.2 \times 10^3$ LSK cells in 3A/p53$^{+/-}$ mice compared with 2.9×10^5 LSK cells in wild-type mice.

In addition to life-span extension, a p53-null mutation also alleviated the developmental defect of lymphocytes in DNA-PKcs$^{3A/3A}$ mice. Thymocyte cell numbers were partially rescued (60% of wild-type mice) in 3A/p53$^{-/-}$ mice but not in 3A/p53$^{+/-}$ mice (Fig. 5 E), and the distribution of CD4 versus CD8 cells was normalized in 3A/p53$^{-/-}$ thymocytes (Fig. S4 B). The rescue of B cell development was also obvious, as the numbers of B cells in 3A/p53$^{-/-}$ mice were completely normal in bone marrow (Fig. 5 F) but restored to a lesser degree in the spleen (Fig. 5 G). Furthermore, even with the loss of a single p53 gene, the numbers of B cells were partially rescued. There were very few B220$^+$IgM$^+$ mature B cells in the 3A/p53$^{+/+}$ bone marrow, but these cells were clearly detectable in 3A/p53$^{-/-}$ mice (Fig. S4 C). Thus, in contrast to DNA-PKcs–deficient SCID mice in which loss of p53 does not rescue B cell development (Nacht et al., 1996), there is partial rescue of B lymphocytes in 3A/p53$^{-/-}$ mice. This also suggests that the V(D)J recombination defect in DNA-PKcs$^{3A/3A}$ mice is less severe than in the complete absence of DNA-PKcs.

Increase of genotoxic stress in the intestinal crypt and epidermis

In addition to HSC loss, elevation of the p53-dependent genotoxic stress response in DNA-PKcs$^{3A/3A}$ mice was also evident in the intestinal crypt and epidermis. The intestinal crypt is the proliferation compartment and contains intestine stem cells, which give rise to different intestine epithelial cells for intestinal homeostasis maintenance. Immunohistological analysis revealed that a significant increase of TUNEL-positive cells was found in the intestinal crypt of DNA-PKcs$^{3A/3A}$ mice and that the p53-null mutation alleviated the defect completely (Fig. 6 A). Skin hyperpigmentation is another example of a p53-dependent stress response (McGowan et al., 2008) and can be found in the footpad and tail of DNA-PKcs$^{3A/3A}$ mice (Fig. 6, B and C). As expected, the hyperpigmentation phenotype is completely reversed in 3A/p53$^{-/-}$ mice. Footpad hyperpigmentation became apparent in DNA-PKcs$^{3A/3A}$ mice as early as 1 wk after birth and

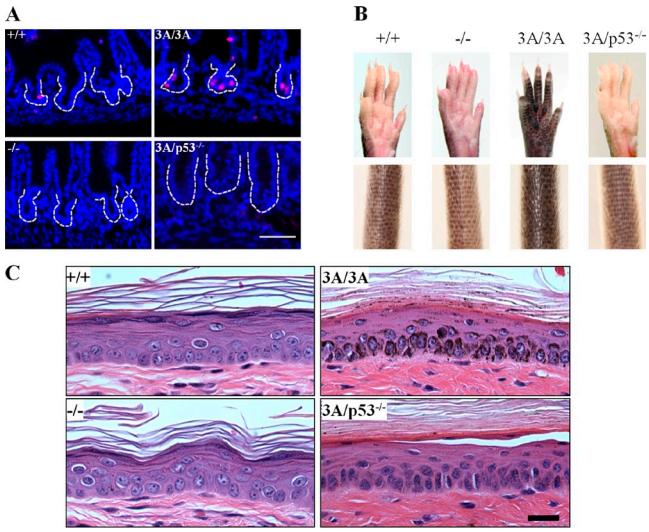

Figure 6. **Activation of p53 in the intestinal crypt and epidermis in DNA-PKcs$^{3A/3A}$ mice.** (A) Representative figures of a TUNEL assay. Increase of TUNEL-positive apoptotic cells (red) in the DNA-PKcs$^{3A/3A}$ intestinal crypt (outlined with dashed lines). Nuclei were counterstained with DAPI (blue). Bar, 50 µm. (B) Skin hyperpigmentation is clearly distinguishable in the DNA-PKcs$^{3A/3A}$ footpad and tail. (C) Hematoxylin and eosin staining of tail skin section. Massive melanin accumulated in the DNA-PKcs$^{3A/3A}$ epidermis and was abolished in a p53-null background. Bar, 20 µm.

was further darkened with age. In contrast, there was no footpad pigmentation in wild-type and heterozygotic pups, whereas mild footpad pigmentation could also be found in older (>2 mo) heterozygotic mice (unpublished data).

Hypersensitivity of DNA-PKcs$^{3A/3A}$ MEFs to DNA cross-linking agents

DNA-PKcs$^{3A/3A}$ MEFs exhibit a similar radiosensitivity to DNA-PKcs$^{-/-}$ MEFs and defective V(D)J recombination, yet only in DNA-PKcs$^{3A/3A}$ mice is there a block in hematopoiesis and an activation of the p53 pathway. Thus, there are likely to be defects in addition to impaired NHEJ. To test this possibility, DNA-PKcs$^{3A/3A}$ MEFs were subjected to different DNA damage agents (Fig. 7 A and Fig. S5 A). Clonogenic survival analyses revealed that DNA-PKcs$^{3A/3A}$ MEFs displayed a greater sensitivity toward replication stress inducers, including UV irradiation, camptothecin, and mitomycin C (MMC; Fig. 7 A). The most striking difference came from treatment with the DNA cross-linking agent MMC, as clonogenic survival of DNA-PKcs$^{3A/3A}$ MEFs was dramatically reduced, whereas heterozygotic MEFs and, importantly, DNA-PKcs$^{-/-}$ MEFs were not affected. Furthermore, MMC treatment induced a significant increase in chromosome aberrations in DNA-PKcs$^{3A/3A}$ MEFs (Fig. 7 B), among which radial structures were frequently observed (Fig. S5 B).

Hypersensitivity toward DNA cross-linking agents and bone marrow failure are the hallmarks of the inherited human disease FA. The repair of DNA interstrand cross-links is a complex process that involves the FA complex and the HR pathway (Mirchandani and D'Andrea, 2006). To determine whether the FA pathway was affected, we analyzed the induction of FANCD2 monoubiquitination in response to DNA damage. Immunoblotting revealed that FANCD2 monoubiquitination was attenuated in DNA-PKcs$^{3A/3A}$ MEFs in response to IR and MMC (Fig. 7 C and Fig. S5 D) but was not ablated as observed in FANCA$^{-/-}$ MEFs (Fig. S5 E). This attenuation is not likely caused by a reduced S-phase population in DNA-PKcs$^{3A/3A}$ MEFs, as no clear difference exists in cell cycle redistribution between wild-type and DNA-PKcs$^{3A/3A}$ MEFs (Fig. S5 C). Activated FANCD2 is recruited to chromatin and forms nuclear foci where it facilitates HR and interstrand cross-link repair (Garcia-Higuera et al., 2001). In response to IR treatment, FANCD2 foci formation was detected in wild-type cells as early as 20 min after irradiation (unpublished data), and the percentage of cells with FANCD2 foci increases with time (Fig. 7 D). In contrast, FANCD2 foci in DNA-PKcs$^{3A/3A}$ MEFs appeared with delayed kinetics, and the percentage of cells with foci was ~50% of wild-type MEFs at various time points after IR. A similar defect was detected in the formation of Rad51 nuclear foci (Fig. S5 F), a prerequisite of HR-mediated DNA repair (Haaf et al., 1995). Formation of Rad51 foci was attenuated in DNA-PKcs$^{3A/3A}$ MEFs but was enhanced in DNA-PKcs$^{-/-}$ MEFs, which is likely because of the elevation of HR activity in the absence of NHEJ (Allen et al., 2002). Finally, we analyzed HR activity using the direct repeat (DR)–GFP reporter approach (Pierce et al., 1999). MEFs with a single integration of the DR-GFP reporter were transfected with an ISceI- glucocorticoid receptor (GR)–RFP construct to induce DSB formation and HR reaction (Soutoglou et al., 2007). Our result revealed that HR activity was attenuated in DNA-PKcs$^{3A/3A}$ MEFs, and a significant portion of ISceI-GR-RFP–expressing (RFP^{+}) DNA-PKcs$^{3A/3A}$ cells was GFP^{-} (no recombination) as compared with wild-type MEFs (Fig. 7 E). In contrast, HR activity was further enhanced in DNA-PKcs$^{-/-}$ MEFs because of a lack of NHEJ activity. The negative impact of the DNA-PKcs^{3A} mutant on the HR/FA responses thus provides an explanation for the phenotypical difference between DNA-PKcs$^{3A/3A}$ mice and DNA-PKcs–null mice.

Discussion

The self-renewal property of HSCs and their ability to sustain long-term hematopoiesis require that genome integrity is strictly maintained (Kenyon and Gerson, 2007; Niedernhofer, 2008). It is well characterized that hematopoietic cells are highly sensitive to radiation-induced DNA damage, and bone marrow aplasia is one of main causes for radiation-induced lethality. A recent study showed that HSCs, but not progenitor cells, are preferentially killed by radiation, suggesting that HSCs are among the most sensitive cell types to DNA damage (Wang et al., 2006). HSCs in DNA repair-deficient individuals are highly susceptible to various kinds of genotoxic stresses. Genetically modified mouse models also revealed that defects in the DNA damage response result in the dysfunction of HSC maintenance. Hematopoietic failure with an early development of bone marrow hypocellularity is manifested in mice with a hypomorphic mutation of Rad50 (Rad50$^{S/S}$; Bender et al., 2002) and mice knockout of ERCC1, a key factor in nucleotide excision repair and interstrand cross-link repair (Niedernhofer et al., 2004; Prasher et al., 2005). Deficiency of ATM leads to elevated levels of oxidative

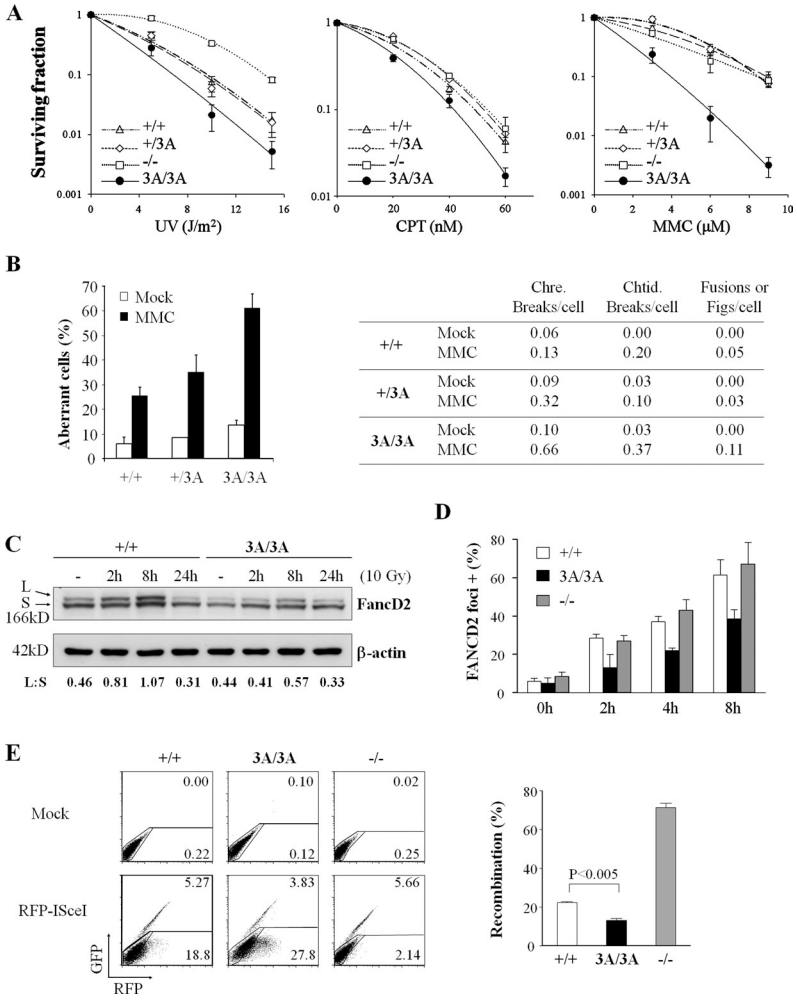

		Chre. Breaks/cell	Chtid. Breaks/cell	Fusions or Figs/cell
+/+	Mock	0.06	0.00	0.00
	MMC	0.13	0.20	0.05
+/3A	Mock	0.09	0.03	0.00
	MMC	0.32	0.10	0.03
3A/3A	Mock	0.10	0.03	0.00
	MMC	0.66	0.37	0.11

Figure 7. **Defect in multiple DNA repair pathways in DNA-PKcs$^{3A/3A}$ cells.** (A) Clonogenic survival of SV40-transformed MEFs after UV irradiation, camptothecin (CPT), and mitomycin C (MMC). Representative data of three independent assays are shown. (B) Increase of MMC-induced chromosomal aberrations in DNA-PKcs$^{3A/3A}$ MEFs from two independent experiments. (left) Percentages of MEFs harboring chromosomal aberrations with or without MMC treatment. (right) The average numbers of chromosome (Chre.) or chromatid (Chtid.) breaks and chromosomal fusions were calculated from ≥50 mitotic spreads of each genotype. (C) FANCD2 monoubiquitination after IR treatment. Primary MEF cultures were subjected to 10 Gy of γ-ray and were harvested at the indicated time points for Western blotting. The ratios between mono- (L) and unubiquitinated (S) FANCD2 are shown. (D) FANCD2 nuclear foci formation after IR (5 Gy) treatment. Percentages of FANCD2 foci-positive cells (more than five foci) at different time points were analyzed from two independent assays. Greater than 200 cells were counted for each time point and genotype. (E) Measurement of HR with a DR-GFP assay. MEFs with a single copy of the DR-GFP HR reporter were mock transfected or transfected with the ISceI-GR-RFP plasmid and were analyzed at 24 h. Lines divided the cells into three populations. The bottom left cell population is negative for both RFP and GFP; the bottom right cell population is only RFP positive. The top cell population is positive for both RFP and GFP. The numbers indicate percentages of cells in each gate. Recombination was determined by the fraction of GFP$^+$ cells among all GFP$^+$ and RFP$^+$ cells. Each point represents data from three individual clones. Error bars represent SD.

stress and a progressive loss of the HSC pool with age (Ito et al., 2004). Similarly, NHEJ deficiency in Ku80 knockout mice diminishes HSC self-renewal capacity, whereas hypomorphic Lig4^{Y288C} mice display an age-dependent decrease in HSC numbers and bone marrow cellularity (Nijnik et al., 2007; Rossi et al., 2007). In contrast, HSC loss in DNA-PKcs$^{3A/3A}$ mice occurs significantly earlier during embryonic development, which resembles Rad50$^{S/S}$ and ERCC1$^{-/-}$ models, though it is not clear whether there is a functional overlap between the DNA-PKcs^{3A} mutant protein and these two DNA repair factors in terms of HSC maintenance. On the other hand, complete DNA-PKcs deficiency leads to a decrease in HSC number (unpublished data) and repopulating ability in aged DNA-PKcs knockout mice. The distinct phenotypes in HSC maintenance between DNA-PKcs knockout and knockin mice is likely a result of their difference in DSB repair capacity, as DNA-PKcs$^{3A/3A}$ cells are also defective in the HR/FA responses in addition to the diminished NHEJ activity. Thus, the combined deficiency in DSB repair renders DNA-PKcs$^{3A/3A}$ cells hypersensitive to MMC and other replication stress agents. It is conceivable that the HR/FA mechanism, but not the NHEJ, is essential for replication-associated DNA damage repair and is critical for the rapid expansion of HSC populations in developing fetal liver.

DSBs are among the most dangerous types of DNA lesions and pose a great challenge to cellular survival and genome integrity maintenance. Multiple repair mechanisms, including NHEJ, HR, and additional backup pathways, have evolved to ensure that DSBs are promptly and properly eliminated from the genome. Outside V(D)J recombination events, endogenous DSBs occur primarily in the cycling cells though the conversion of single-strand lesions during replication (Vilenchik and Knudson, 2003). From the standpoint of endogenous DSB production, we could assume that DNA-PK and its downstream NHEJ pathway, which is the predominant DSB repair mechanism in mammalian cells and is operational in all cell cycle phases, have a greater involvement in the replication-associated DNA damage response than we previously thought. However, it is not clear how DNA-PKcs and other factors of DSB repair are coordinated in response to replicative stresses, particularly in the highly proliferative cell population. Our unexpected findings from the DNA-PKcs^{3A} mouse model provide strong evidence that the impact of DNA-PKcs, particularly its phosphorylation at the mouse Thr2605 cluster (human Thr2609), has a role beyond the NHEJ mechanism.

It recently became clear that the competition between the NHEJ and the HR/FA pathway has important biological significance. For example, loss of the NHEJ factor 53BP1 alleviates

the hypersensitivity of HR-defective Brca1 mutant cells to DNA-damaging agents and restores DSB repair by HR (Bouwman et al., 2010; Bunting et al., 2010). In addition, the FA pathway plays a critical role in eliminating toxic NHEJ; suppression of NHEJ alleviates the sensitivity of FA mutant cells to DNA cross-linking agents and facilitates error-free repair by HR (Adamo et al., 2010; Pace et al., 2010). Similarly, our data suggest that the DNA-PKcs^{3A} mutant protein interferes with the HR pathway, which could explain the sensitivity to replication damage and the severity of hematopoietic failure.

We have previously reported that the human Thr2609 cluster is phosphorylated directly by the ATR kinase upon replication stress (Yajima et al., 2006). This ATR-dependent DNA-PKcs phosphorylation virtually facilitates processing of replication-associated DNA lesions through the HR/FA machinery. It is likely that, in such a repair process, the shift from error-prone end joining to faithful repair by the HR/FA is partially achieved by ATR-dependent DNA-PKcs phosphorylation. In support of this, a similar stem cell defect was observed in conditional ATR knockout mice (Ruzankina et al., 2007). It is not clear yet how DNA-PKcs phosphorylation at the Thr2609 cluster promotes HR/FA activities. One possible explanation is that Thr2609 cluster phosphorylation changes the conformation of DSB-bound DNA-PKcs and releases DSB ends to the HR/FA machineries (Meek et al., 2008).

The loss of HSCs in DNA-PKcs$^{3A/3A}$ mice is primarily caused by p53-mediated apoptotic response, as the p53-null mutation reinstates HSC reserves in DNA-PKcs$^{3A/3A}$ mice. In addition to HSC loss, elevation of genotoxic stress and p53 activation was found in other proliferating tissues as evident from intestinal crypt cell apoptosis and epidermal hyperpigmentation. These results reiterate that DNA-PKcs phosphorylation at the human Thr2609/mouse Thr2605 cluster is critical for replication stress response and the maintenance of tissue homeostasis. The tissue-specific outcome of genotoxic stress imposed by the DNA-PKcs^{3A} mutant protein or DNA-PKcs dysfunction may depend on cell type–specific apoptosis/senescence and the compensation capacity from varied sizes of stem cell pools in different tissues and organs.

Gene mutations in the FA protein complex and HR components have been indentified in human FA syndrome characterized by congenital bone marrow failure, short stature, abnormal skin pigmentation, reduced fertility, hypersensitivity toward DNA cross-link damages, and increased genomic instability (Moldovan and D'Andrea, 2009). The mechanism underlying the clinical findings of FA remains unclear, given the fact that none of the current mouse models for HR and FA systematically recapitulated these pathophysiological changes. It is interesting to note that the DNA-PKcs$^{3A/3A}$ mouse resembles human FA syndromes more than FA mouse models. The hallmarks of FA, including aplastic anemia, abnormal skin pigmentation, MMC sensitivity, and radial chromosome formation with MMC treatment, are all observed in DNA-PKcs$^{3A/3A}$ mice, suggesting that, in human patients, FA mutations also likely affect the stem cell compartment during embryo development and activate p53, which generates pathological changes in multiple organs. Indeed, p53 has also been shown to be up-regulated in FA cells, and it has been speculated that the p53-dependent apoptotic pathway may contribute to the loss of stem cells in bone marrow (Kennedy and D'Andrea, 2005; Rani et al., 2008). It is interesting to note that the human dyskeratosis congenita syndrome, which is caused by telomerase mutations, also displays bone marrow failure and hyper skin pigmentation characters. Conversely, mice with combined mutations on telomerase and Pot1b, a component of the telomere-protecting shelterin complex, exhibit dyskeratosis congenita–like characteristics, including bone marrow failure and footpad hyperpigmentation (Hockemeyer et al., 2008; He et al., 2009). This similarity to DNA-PKcs$^{3A/3A}$ mice suggests a common stress response among different congenital bone marrow failure diseases and warrants further investigation of DNA-PKcs phosphorylation on telomere maintenance.

Materials and methods

Construction of the targeting vector and generation of DNA-PKcs$^{3A/3A}$ knockin mice

The 3A knockin targeting vector was constructed using a previously described self-excision gene-targeting approach (Bunting et al., 1999). The DNA-PKcs^{3A} mice were maintained in the mixed genetic background of 129× C57BL/6 and were bred with p53-null mice in an FVB background. ES cell targeting and generation of chimeric mice were performed at the transgenic core facility at the University of Texas Southwestern Medical Center. All animal experimental protocols were approved by the Animal Care Committee of the University of Texas Southwestern Medical Center.

Clonogenic survival and chromosomal aberrations

Primary and SV40-transformed MEFs from E13.5 embryos were cultured in α minimum essential medium supplemented with 10% fetal calf serum and penicillin/streptomycin. MEFs were maintained in a 37°C humidified atmosphere with 3% O_2 and 10% CO_2. For clonogenic survival, SV40-transformed MEFs were treated with different doses of mutagens and were trypsinized/reseeded in appropriate numbers in 10-cm tissue-culture dishes for 7 d. For chromosomal aberrations, primary MEFs (passages 2–5) were incubated with 40 nM MMC for 24 h and 0.1 mg/ml colcemid in the last 2 h.

Fluorescence-activated cell sorting and ex vivo expansion of HSCs

Thymus, bone marrow, or fetal liver single-cell suspensions were stained with the indicated antibodies and analyzed using either a FACSCalibur (BD) or LSRII (BD) flow cytometer (Huynh et al., 2008). HSCs were sorted using a flow cytometer (FACSAria; BD) essentially as previously described (Huynh et al., 2008). For apoptosis analysis, cell suspensions were stained with phycoerythrin-anti–Annexin V (BD). Ex vivo expansion of fetal liver HSCs was performed using a previously published protocol (Zhang and Lodish, 2004).

V(D)J recombination assay

Dδ2:Jδ1 coding joint junctions were PCR amplified from total thymocyte DNA using a nested amplification protocol. The PCR conditions and primer design are detailed in Fig. S2.

Bone marrow/HSC transplantation and competitive repopulating assay

Total bone marrow cells (5×10^5) or $Lin^-Sca\text{-}1^+c\text{-}Kit^+$ cells (1,500–5,000) from wild-type littermates were injected into the retro-orbital plexus of 2- or 3-wk-old DNA-PKcs$^{3A/3A}$ mice without preconditioning. Competitive repopulation was performed using wild-type, DNA-PKcs$^{3A/3A}$, or DNA-PKcs$^{-/-}$ cells (CD45.2 background), mixed with competitive bone marrow cells from B6-LY5.2/Cr mice (CD45.1 background), and injected into lethally irradiated (5 Gy × 2) B6-LY5.2/Cr–recipient mice. 2 mo after injection, populations of $CD45.1^+$ and $CD45.2^+$ peripheral blood cells were analyzed by flow cytometry.

DR-GFP HR assay

SV40-transformed MEFs with single-copy incorporation of the DR-GFP reporter (Pierce et al., 1999) were transfected with the ISceI-GR-RFP plasmid (Addgene) and treated with 10 nM triamcinolone acetonide for 24 h followed by flow cytometry analysis. HR activities were determined by the percentage of GFP^+RFP^+ double-positive cells among all ISceI-GR-RFP–expressing (RFP^+) cells.

Online supplemental material

Fig. S1 shows a DNA-PKcs^{3A} mouse model with three alanine substitutions at the Thr2605 cluster of the endogenous *DNA-PKcs* gene. Fig. S2 shows compromised lymphocyte development in DNA-PKcs$^{3A/3A}$ mice. Fig. S3 shows BMT rescue of hematopoietic defects in DNA-PKcs$^{3A/3A}$ mice. Fig. S4 shows spontaneous DNA damage and a p53 signaling pathway in DNA-PKcs$^{3A/3A}$ cells. Fig. S5 shows DNA repair defects in DNA-PKcs$^{3A/3A}$ cells. Table S1 shows Dδ2:Jδ1 coding joint junctions cloned and sequenced from wild-type mice. Table S2 shows Dδ2:Jδ1 coding joint junctions cloned and sequenced from DNA-PKcs–deficient SCID mice. Table S3 shows Dδ2:Jδ1 coding joint junctions cloned and sequenced from DNA-PKcs$^{3A/3A}$ mice. Table S4 shows the peripheral blood cell count of 2-wk-old mice. Online supplemental material is available at http://www.jcb.org/cgi/content/full/jcb.201009074/DC1.

We thank Drs. K.R. Thomas and M.R. Capecchi for providing the ACN plasmid, Drs. D. Boothman and T. Mashimo for providing p53 knockout mice, Dr. A. D'Andrea for providing the anti-FANCD2 antibody, and Dr. M. Digweed for FANCA$^{-/-}$ MEFs. We thank Robert E. Silvany for cell-sorting work and Carolyn Spanial, Eric Shih, Francisca Ahn, and Joyce Wang for mouse breeding.

B.P.C. Chen is supported by National Aeronautics and Space Administration grant NNX07AP84G, D.J. Chen is supported by National Institutes of Health grant CA50519, and C.C. Zhang is supported by National Institutes of Health grant CA120099, the Michael. L. Rosenberg Endowed Scholar Fund, the American Cancer Society, the American Society of Hematology Junior Faculty Award, the Robert A. Welch Foundation, and the Basil O'Connor Starter Scholar Award from the March of Dimes Foundation.

Submitted: 14 September 2010
Accepted: 22 March 2011

References

Adamo, A., S.J. Collis, C.A. Adelman, N. Silva, Z. Horejsi, J.D. Ward, E. Martinez-Perez, S.J. Boulton, and A. La Volpe. 2010. Preventing non-homologous end joining suppresses DNA repair defects of Fanconi anemia. *Mol. Cell*. 39:25–35. doi:10.1016/j.molcel.2010.06.026

Allen, C., A. Kurimasa, M.A. Brenneman, D.J. Chen, and J.A. Nickoloff. 2002. DNA-dependent protein kinase suppresses double-strand break-induced and spontaneous homologous recombination. *Proc. Natl. Acad. Sci. USA*. 99:3758–3763. doi:10.1073/pnas.052545899

Bender, C.F., M.L. Sikes, R. Sullivan, L.E. Huye, M.M. Le Beau, D.B. Roth, O.K. Mirzoeva, E.M. Oltz, and J.H. Petrini. 2002. Cancer predisposition and hematopoietic failure in Rad50(S/S) mice. *Genes Dev.* 16:2237–2251. doi:10.1101/gad.1007902

Bouwman, P., A. Aly, J.M. Escandell, M. Pieterse, J. Bartkova, H. van der Gulden, S. Hiddingh, M. Thanasoula, A. Kulkarni, Q. Yang, et al. 2010. 53BP1 loss rescues BRCA1 deficiency and is associated with triple-negative and BRCA-mutated breast cancers. *Nat. Struct. Mol. Biol.* 17:688–695. doi:10.1038/nsmb.1831

Bunting, M., K.E. Bernstein, J.M. Greer, M.R. Capecchi, and K.R. Thomas. 1999. Targeting genes for self-excision in the germ line. *Genes Dev.* 13:1524–1528. doi:10.1101/gad.13.12.1524

Bunting, S.F., E. Callén, N. Wong, H.T. Chen, F. Polato, A. Gunn, A. Bothmer, N. Feldhahn, O. Fernandez-Capetillo, L. Cao, et al. 2010. 53BP1 inhibits homologous recombination in Brca1-deficient cells by blocking resection of DNA breaks. *Cell*. 141:243–254. doi:10.1016/j.cell.2010.03.012

Callén, E., M. Jankovic, N. Wong, S. Zha, H.T. Chen, S. Difilippantonio, M. Di Virgilio, G. Heidkamp, F.W. Alt, A. Nussenzweig, and M. Nussenzweig. 2009. Essential role for DNA-PKcs in DNA double-strand break repair and apoptosis in ATM-deficient lymphocytes. *Mol. Cell*. 34:285–297. doi:10.1016/j.molcel.2009.04.025

Chan, D.W., B.P. Chen, S. Prithivirajsingh, A. Kurimasa, M.D. Story, J. Qin, and D.J. Chen. 2002. Autophosphorylation of the DNA-dependent protein kinase catalytic subunit is required for rejoining of DNA double-strand breaks. *Genes Dev.* 16:2333–2338. doi:10.1101/gad.1015202

Chen, B.P., D.W. Chan, J. Kobayashi, S. Burma, A. Asaithamby, K. Morotomi-Yano, E. Botvinick, J. Qin, and D.J. Chen. 2005. Cell cycle dependence of DNA-dependent protein kinase phosphorylation in response to DNA double strand breaks. *J. Biol. Chem.* 280:14709–14715. doi:10.1074/jbc.M408827200

Chen, B.P., N. Uematsu, J. Kobayashi, Y. Lerenthal, A. Krempler, H. Yajima, M. Löbrich, Y. Shiloh, and D.J. Chen. 2007. Ataxia telangiectasia mutated (ATM) is essential for DNA-PKcs phosphorylations at the Thr-2609 cluster upon DNA double strand break. *J. Biol. Chem.* 282:6582–6587. doi:10.1074/jbc.M611605200

Cook, A.J., L. Oganesian, P. Harumal, A. Basten, R. Brink, and C.J. Jolly. 2003. Reduced switching in SCID B cells is associated with altered somatic mutation of recombined S regions. *J. Immunol.* 171:6556–6564.

Difilippantonio, S., E. Gapud, N. Wong, C.Y. Huang, G. Mahowald, H.T. Chen, M.J. Kruhlak, E. Callen, F. Livak, M.C. Nussenzweig, et al. 2008. 53BP1 facilitates long-range DNA end-joining during V(D)J recombination. *Nature*. 456:529–533. doi:10.1038/nature07476

Ding, Q., Y.V. Reddy, W. Wang, T. Woods, P. Douglas, D.A. Ramsden, S.P. Lees-Miller, and K. Meek. 2003. Autophosphorylation of the catalytic subunit of the DNA-dependent protein kinase is required for efficient end processing during DNA double-strand break repair. *Mol. Cell. Biol.* 23:5836–5848. doi:10.1128/MCB.23.16.5836-5848.2003

Douglas, P., G.P. Sapkota, N. Morrice, Y. Yu, A.A. Goodarzi, D. Merkle, K. Meek, D.R. Alessi, and S.P. Lees-Miller. 2002. Identification of in vitro and in vivo phosphorylation sites in the catalytic subunit of the DNA-dependent protein kinase. *Biochem. J.* 368:243–251. doi:10.1042/BJ20020973

Gao, Y., J. Chaudhuri, C. Zhu, L. Davidson, D.T. Weaver, and F.W. Alt. 1998. A targeted DNA-PKcs-null mutation reveals DNA-PK-independent functions for KU in V(D)J recombination. *Immunity*. 9:367–376. doi:10.1016/S1074-7613(00)80619-6

Garcia-Higuera, I., T. Taniguchi, S. Ganesan, M.S. Meyn, C. Timmers, J. Hejna, M. Grompe, and A.D. D'Andrea. 2001. Interaction of the Fanconi anemia proteins and BRCA1 in a common pathway. *Mol. Cell*. 7:249–262. doi:10.1016/S1097-2765(01)00173-3

Gu, Y., K.J. Seidl, G.A. Rathbun, C. Zhu, J.P. Manis, N. van der Stoep, L. Davidson, H.L. Cheng, J.M. Sekiguchi, K. Frank, et al. 1997. Growth retardation and leaky SCID phenotype of Ku70-deficient mice. *Immunity*. 7:653–665. doi:10.1016/S1074-7613(00)80386-6

Haaf, T., E.I. Golub, G. Reddy, C.M. Radding, and D.C. Ward. 1995. Nuclear foci of mammalian Rad51 recombination protein in somatic cells after DNA damage and its localization in synaptonemal complexes. *Proc. Natl. Acad. Sci. USA*. 92:2298–2302. doi:10.1073/pnas.92.6.2298

He, H., Y. Wang, X. Guo, S. Ramchandani, J. Ma, M.F. Shen, D.A. Garcia, Y. Deng, A.S. Multani, M.J. You, and S. Chang. 2009. Pot1b deletion and telomerase haploinsufficiency in mice initiate an ATR-dependent DNA damage response and elicit phenotypes resembling dyskeratosis congenita. *Mol. Cell. Biol.* 29:229–240. doi:10.1128/MCB.01400-08

Hockemeyer, D., W. Palm, R.C. Wang, S.S. Couto, and T. de Lange. 2008. Engineered telomere degradation models dyskeratosis congenita. *Genes Dev.* 22:1773–1785. doi:10.1101/gad.1679208

Huynh, H., S. Iizuka, M. Kaba, O. Kirak, J. Zheng, H.F. Lodish, and C.C. Zhang. 2008. Insulin-like growth factor-binding protein 2 secreted by a tumorigenic cell line supports ex vivo expansion of mouse hematopoietic stem cells. *Stem Cells*. 26:1628–1635. doi:10.1634/stemcells.2008-0064

Ito, K., A. Hirao, F. Arai, S. Matsuoka, K. Takubo, I. Hamaguchi, K. Nomiyama, K. Hosokawa, K. Sakurada, N. Nakagata, et al. 2004. Regulation of oxidative stress by ATM is required for self-renewal of haematopoietic stem cells. *Nature*. 431:997–1002. doi:10.1038/nature02989

Kennedy, R.D., and A.D. D'Andrea. 2005. The Fanconi Anemia/BRCA pathway: new faces in the crowd. *Genes Dev.* 19:2925–2940. doi:10.1101/gad.1370505

Kenyon, J., and S.L. Gerson. 2007. The role of DNA damage repair in aging of adult stem cells. *Nucleic Acids Res.* 35:7557–7565. doi:10.1093/nar/gkm1064

Kondo, M., A.J. Wagers, M.G. Manz, S.S. Prohaska, D.C. Scherer, G.F. Beilhack, J.A. Shizuru, and I.L. Weissman. 2003. Biology of hematopoietic stem cells and progenitors: implications for clinical application. *Annu. Rev. Immunol.* 21:759–806. doi:10.1146/annurev.immunol.21.120601.141007

Kurimasa, A., H. Ouyang, L.J. Dong, S. Wang, X. Li, C. Cordon-Cardo, D.J. Chen, and G.C. Li. 1999. Catalytic subunit of DNA-dependent protein kinase: impact on lymphocyte development and tumorigenesis. *Proc. Natl. Acad. Sci. USA*. 96:1403–1408. doi:10.1073/pnas.96.4.1403

Ma, Y., U. Pannicke, H. Lu, D. Niewolik, K. Schwarz, and M.R. Lieber. 2005. The DNA-dependent protein kinase catalytic subunit phosphorylation sites in human Artemis. *J. Biol. Chem.* 280:33839–33846. doi:10.1074/jbc.M507113200

Manis, J.P., D. Dudley, L. Kaylor, and F.W. Alt. 2002. IgH class switch recombination to IgG1 in DNA-PKcs-deficient B cells. *Immunity*. 16:607–617. doi:10.1016/S1074-7613(02)00306-0

McGowan, K.A., J.Z. Li, C.Y. Park, V. Beaudry, H.K. Tabor, A.J. Sabnis, W. Zhang, H. Fuchs, M.H. de Angelis, R.M. Myers, et al. 2008. Ribosomal mutations cause p53-mediated dark skin and pleiotropic effects. *Nat. Genet.* 40:963–970. doi:10.1038/ng.188

Meek, K., P. Douglas, X. Cui, Q. Ding, and S.P. Lees-Miller. 2007. trans Autophosphorylation at DNA-dependent protein kinase's two major autophosphorylation site clusters facilitates end processing but not end joining. *Mol. Cell. Biol.* 27:3881–3890. doi:10.1128/MCB.02366-06

Meek, K., V. Dang, and S.P. Lees-Miller. 2008. DNA-PK: the means to justify the ends? *Adv. Immunol.* 99:33–58. doi:10.1016/S0065-2776(08)00602-0

Mikkola, H.K., and S.H. Orkin. 2006. The journey of developing hematopoietic stem cells. *Development*. 133:3733–3744. doi:10.1242/dev.02568

Mirchandani, K.D., and A.D. D'Andrea. 2006. The Fanconi anemia/BRCA pathway: a coordinator of cross-link repair. *Exp. Cell Res.* 312:2647–2653. doi:10.1016/j.yexcr.2006.06.014

Moldovan, G.L., and A.D. D'Andrea. 2009. How the fanconi anemia pathway guards the genome. *Annu. Rev. Genet.* 43:223–249. doi:10.1146/annurev-genet-102108-134222

Morrison, S.J., H.D. Hemmati, A.M. Wandycz, and I.L. Weissman. 1995. The purification and characterization of fetal liver hematopoietic stem cells. *Proc. Natl. Acad. Sci. USA*. 92:10302–10306. doi:10.1073/pnas.92.22.10302

Nacht, M., A. Strasser, Y.R. Chan, A.W. Harris, M. Schlissel, R.T. Bronson, and T. Jacks. 1996. Mutations in the p53 and SCID genes cooperate in tumorigenesis. *Genes Dev.* 10:2055–2066. doi:10.1101/gad.10.16.2055

Niedernhofer, L.J. 2008. DNA repair is crucial for maintaining hematopoietic stem cell function. *DNA Repair (Amst.)*. 7:523–529. doi:10.1016/j.dnarep.2007.11.012

Niedernhofer, L.J., H. Odijk, M. Budzowska, E. van Drunen, A. Maas, A.F. Theil, J. de Wit, N.G. Jaspers, H.B. Beverloo, J.H. Hoeijmakers, and R. Kanaar. 2004. The structure-specific endonuclease Ercc1-Xpf is required to resolve DNA interstrand cross-link-induced double-strand breaks. *Mol. Cell. Biol.* 24:5776–5787. doi:10.1128/MCB.24.13.5776-5787.2004

Nijnik, A., L. Woodbine, C. Marchetti, S. Dawson, T. Lambe, C. Liu, N.P. Rodrigues, T.L. Crockford, E. Cabuy, A. Vindigni, et al. 2007. DNA repair is limiting for haematopoietic stem cells during ageing. *Nature*. 447:686–690. doi:10.1038/nature05875

Nussenzweig, A., C. Chen, V. da Costa Soares, M. Sanchez, K. Sokol, M.C. Nussenzweig, and G.C. Li. 1996. Requirement for Ku80 in growth and immunoglobulin V(D)J recombination. *Nature*. 382:551–555. doi:10.1038/382551a0

Ouyang, H., A. Nussenzweig, A. Kurimasa, V.C. Soares, X. Li, C. Cordon-Cardo, W. Li, N. Cheong, M. Nussenzweig, G. Iliakis, et al. 1997. Ku70 is required for DNA repair but not for T cell antigen receptor gene recombination in vivo. *J. Exp. Med.* 186:921–929. doi:10.1084/jem.186.6.921

Pace, P., G. Mosedale, M.R. Hodskinson, I.V. Rosado, M. Sivasubramaniam, and K.J. Patel. 2010. Ku70 corrupts DNA repair in the absence of the Fanconi anemia pathway. *Science*. 329:219–223. doi:10.1126/science.1192277

Pierce, A.J., R.D. Johnson, L.H. Thompson, and M. Jasin. 1999. XRCC3 promotes homology-directed repair of DNA damage in mammalian cells. *Genes Dev.* 13:2633–2638. doi:10.1101/gad.13.20.2633

Prasher, J.M., A.S. Lalai, C. Heijmans-Antonissen, R.E. Ploemacher, J.H. Hoeijmakers, I.P. Touw, and L.J. Niedernhofer. 2005. Reduced hematopoietic reserves in DNA interstrand crosslink repair-deficient Ercc1−/− mice. *EMBO J.* 24:861–871. doi:10.1038/sj.emboj.7600542

Rani, R., J. Li, and Q. Pang. 2008. Differential p53 engagement in response to oxidative and oncogenic stresses in Fanconi anemia mice. *Cancer Res.* 68:9693–9702. doi:10.1158/0008-5472.CAN-08-1790

Rossi, D.J., D. Bryder, J. Seita, A. Nussenzweig, J. Hoeijmakers, and I.L. Weissman. 2007. Deficiencies in DNA damage repair limit the function of haematopoietic stem cells with age. *Nature*. 447:725–729. doi:10.1038/nature05862

Ruzankina, Y., C. Pinzon-Guzman, A. Asare, T. Ong, L. Pontano, G. Cotsarelis, V.P. Zediak, M. Velez, A. Bhandoola, and E.J. Brown. 2007. Deletion of the developmentally essential gene ATR in adult mice leads to age-related phenotypes and stem cell loss. *Cell Stem Cell*. 1:113–126. doi:10.1016/j.stem.2007.03.002

Shiloh, Y. 2003. ATM and related protein kinases: safeguarding genome integrity. *Nat. Rev. Cancer*. 3:155–168. doi:10.1038/nrc1011

Sonoda, E., H. Hochegger, A. Saberi, Y. Taniguchi, and S. Takeda. 2006. Differential usage of non-homologous end-joining and homologous recombination in double strand break repair. *DNA Repair (Amst.)*. 5:1021–1029. doi:10.1016/j.dnarep.2006.05.022

Soutoglou, E., J.F. Dorn, K. Sengupta, M. Jasin, A. Nussenzweig, T. Ried, G. Danuser, and T. Misteli. 2007. Positional stability of single double-strand breaks in mammalian cells. *Nat. Cell Biol.* 9:675–682. doi:10.1038/ncb1591

Taccioli, G.E., A.G. Amatucci, H.J. Beamish, D. Gell, X.H. Xiang, M.I. Torres Arzayus, A. Priestley, S.P. Jackson, A. Marshak Rothstein, P.A. Jeggo, and V.L. Herrera. 1998. Targeted disruption of the catalytic subunit of the DNA-PK gene in mice confers severe combined immunodeficiency and radiosensitivity. *Immunity*. 9:355–366. doi:10.1016/S1074-7613(00)80618-4

Vilenchik, M.M., and A.G. Knudson. 2003. Endogenous DNA double-strand breaks: production, fidelity of repair, and induction of cancer. *Proc. Natl. Acad. Sci. USA*. 100:12871–12876. doi:10.1073/pnas.2135498100

Wang, Y., B.A. Schulte, A.C. LaRue, M. Ogawa, and D. Zhou. 2006. Total body irradiation selectively induces murine hematopoietic stem cell senescence. *Blood*. 107:358–366. doi:10.1182/blood-2005-04-1418

Weterings, E., and D.J. Chen. 2008. The endless tale of non-homologous end-joining. *Cell Res.* 18:114–124. doi:10.1038/cr.2008.3

Yajima, H., K.J. Lee, and B.P. Chen. 2006. ATR-dependent phosphorylation of DNA-dependent protein kinase catalytic subunit in response to UV-induced replication stress. *Mol. Cell. Biol.* 26:7520–7528. doi:10.1128/MCB.00048-06

Zhang, C.C., and H.F. Lodish. 2004. Insulin-like growth factor 2 expressed in a novel fetal liver cell population is a growth factor for hematopoietic stem cells. *Blood*. 103:2513–2521. doi:10.1182/blood-2003-08-2955